Earth Surf. Dynam. Discuss., 2, 535–574, 2014
www.earth-surf-dynam-discuss.net/2/535/2014/
doi:10.5194/esurfd-2-535-2014

Earth Surface Dynamics Discussions
Open Access

Controls on slope-wash erosion rates in the Mojave Desert

O. Crouvi[1,2], V. O. Polyakov[3], J. D. Pelletier[2], and C. Rasmussen[4]

[1]Geological Survey of Israel, 30 Malkhe Israel St., Jerusalem 95501, Israel
[2]Department of Geosciences, University of Arizona, Tucson, AZ 85721, USA
[3]Southwest Watershed Research Center, USDA-ARS, 2000 E. Allen Rd., Tucson, AZ 85719, USA
[4]Department of Soil, Water, and Environmental Science, University of Arizona, Tucson, AZ 85721, USA

Received: 4 May 2014 – Accepted: 2 June 2014 – Published: 18 June 2014

Correspondence to: O. Crouvi (crouvi@gsi.gov.il)

Published by Copernicus Publications on behalf of the European Geosciences Union.

Abstract

This study estimates the rates of soil erosion by slope wash in an arid region and the various factors that control these rates. Decadal-scale erosion rates were estimated on hillslope scales using inventories of ^{137}Cs that were sampled from 46 soil profiles in four different study sites in the Mojave Desert. Calculated mean soil erosion rates per site range from −3.6 to −24.3 t ha^{-1} yr^{-1}. Higher mean rates were associated with gently sloping sites that exhibit low percentage of rock and vegetation coverage, whereas lower mean rates corresponded to steep and rocky sites. Individual erosion rates were not correlated to slope gradient or curvature but were negatively correlated with the volume fraction of rocks in the upper soil profile (i.e., upslope rock coverage). Since the slopes get rockier as they get steeper, any increase in erosion rates with increasing slope is outweighed by the inhibiting effect of greater rock cover. This, together with sandy-loam soil texture on the steep slopes hinders runoff and erosion. Our findings are supported by soil data that show greater heterogeneity in the degree of calcic soil development and higher soluble salt contents in more gently sloping sites that are characterized by high erosion rates. The erosion rates reported here for the gently sloping sites are higher than rates calculated for semi-arid regions, probably due to the lower rock and vegetation coverage in these sites compared to wetter areas. These rates are also higher than millennial-scale rates estimated for the Mojave Desert on watershed scales, and suggest that at least part of the eroded sediments are stored in the adjacent streams and do not reach the piedmonts.

1 Introduction

Quantifying soil erosion rates and processes is essential to understanding how landscapes evolve under climatic, tectonic, and anthropogenic forcing. Although soil erosion is a natural process, it has intensified in the last century mainly due to anthropogenic stressors: each year, ∼ 75 billion metric tons of soil are removed from the land by water

ESURFD
2, 535–574, 2014

and wind erosion, with most coming from agricultural land (Pimentel et al., 1995). Thus, most research effort has been concentrated on agricultural fields, whereas natural, uncultivated regions have been studied less intensively. Rates of soil erosion by water are estimated using different methodologies (e.g., erosion pins, Cesium-137, cosmogenic isotopes) and at different spatial and temporal scales. These rates are relatively well known for semi-arid to humid regions throughout the world (e.g., Lal, 2001; Nearing et al., 2005; Verheijen et al., 2009), but have been less studied in arid environments, especially over decadal time scales.

In arid and semi-arid regions, surface (or slope) wash, induced by overland flow when the rainfall rate exceeds the infiltration capacity, contributes to erosion where vegetation is sparse and hillslope materials are relatively impermeable (Dietrich et al., 2003). Although transport laws for this process are not well established, sediment flux by flowing water is generally a function of both topographic gradient (slope) and contributing area (Dietrich et al., 2003; Dietrich and Perron, 2006). The positive relationship between slope and erosion rate is commonly used to model spatial and temporal changes in soil erosion rates (e.g., the slope-steepness factor in the Universal Soil Loss Equation (USLE) (Wischmeier and Smith, 1978) and its extended form, the Revised Universal Soil Loss Equation (RUSLE) (Renard and Freimund, 1994)). Yet, several field-based studies suggest that the surficial cover on hillslopes might mask the control of slope on erosion rates. For example, a study from the hyper-arid region of Israel found no clear relationship between slope gradient and runoff, but found a negative correlation between slope and erosion (i.e., steeper slopes yield smaller erosion rates) (Yair and Klein, 1973). This inverse relationship was attributed to a difference in the surficial cover of rock fragments. Similar findings were reported from semi-arid sites in southeastern Arizona and the Sierra Nevada, California, showing that overland-flow velocities and erosion rates are only partly controlled by slope gradients, but more importantly are related to differential rock cover (Abrahams and Parsons, 1991; Nearing et al., 1999, 2005; Granger et al., 2001), i.e. as rock coverage increases, soil erosion rate decreases. This relationship is related to the following effects of rock coverage

ESURFD
2, 535–574, 2014

(Poesen et al., 1994): (1) protection against raindrop impact and flow detachment, (2) reduction of physical degradation of the underlying soil, and (3) retardation of flow velocity caused by greater hydraulic roughness associated with the rock cover. In contrast to this negative relationship, studies from an arid region in Israel suggest a positive relationship between erosion and rock coverage, and show that in areas with more pronounced rock coverage, soil erosion increases (Yair and Enzel, 1987; Yair, 1990). Poesen et al. (1994) found that the net effect of rock coverage on soil erosion by water depends on the temporal and spatial scale considered in that a negative relationship exists between sediment yield and percent surficial rock cover at the microplot and macroplot scales (4×10^{-6}–10^{0} m^2 and 10^{1}–10^{4} m^2, respectively). However, at the mesoplot scale (10^{-2}–10^{2} m^2), the relationship between rock coverage and sediment yield is more complex, and can be negative or positive depending on the structure of the topsoil and on the vertical position and size of the rock fragments (Poesen et al., 1994).

Most of the studies that demonstrated the importance of rock cover on soil erosion rates were conducted in semi-arid to humid regions (i.e. those with mean annual precipitation of > 300 mm yr^{-1}). In arid regions (< 200 mm yr^{-1}) our information on processes and rates of soil erosion by water at the hillslope scale is limited (but see Yair and Klein, 1973; Abrahams et al., 1984; Yair, 1990; Owen et al., 2011). In general, arid regions differ from semi-arid regions in how both climatic and surficial properties affect erosion rates. Arid regions are characterized by (1) brief, high-intensity rainfall, (2) large variability in soil thickness and surficial rock cover on a small scale (< 1 m), (3) low vegetation coverage, and (4) high dust accumulation rates. Due to these unique characteristics we cannot directly use the findings of prior studies on soil erosion rates and processes collected in semi-arid to humid regions, to make inferences about arid desert regions. Moreover, the relatively few studies that have estimated water-related erosion in the Mojave Desert focused on millennial-scale erosion rates using cosmogenic nuclides (Nichols et al., 2002, 2007) that represent average rates of large drainage areas.

ESURFD
2, 535–574, 2014

Thus, there is a need to quantify rates of soil erosion by water in arid regions at the hillslope scale.

Inventories of the anthropogenic radioactive cesium-137 ($t_{1/2}$ = 30.2 years) are widely used as tracers of soil movement in a wide range of environments in different regions of the world (e.g., Walling and He, 1999; Nearing et al., 2005; Kaste et al., 2006; O'Farrell et al., 2007). As the only source for ^{137}Cs is nuclear fission (fallout peak in 1963), this fallout nuclide is useful for calculating and tracing soil loss by water over decadal (∼ 50 years) timescales. In this study we used inventories of ^{137}Cs to (1) estimate current decadal-scale soil erosion rates on the hillslope scale in the Mojave Desert, and (2) examine what controls soil erosion rates on hillslopes in arid regions, including topographic parameters, contributing area, surficial rock coverage and vegetation. We hypothesize that (1) erosion rates by overland flow in arid regions could be higher than those in semi-arid regions with otherwise similar slope gradient due to lower vegetation coverage and higher degree of dust accumulation (adding fine dust may decrease infiltration rates and increase runoff), and (2) erosion rates by overland flow in arid regions are mainly controlled by rock coverage, similar to semi-arid regions. We chose four sites in the Ft. Irwin area, CA, that differ in lithology, exhibit a wide range of topographic properties (slope and curvature), and thus serve as a suitable place to examine what variables control the rates of erosion by slope wash. We then compared these erosion rates with soil catena data and with an estimation of millennial-scale erosion rates. Note that as floral bioturbation primarily acts on time scales larger than cycles of growth and death of individual plants, we assume that diffusion-like processes are barely active on short time scales (Kaste et al., 2007) and thus that the decadal-scale soil erosion rates estimated here (using ^{137}Cs inventories) are solely due to slope wash. Erosion by colluvial processes is likely not accounted for in ^{137}Cs inventories.

ESURFD
2, 535–574, 2014

2 Materials and methods

2.1 Study area

The study area is located in the National Training Center at Ft. Irwin, south-central California, in the western Mojave Desert (Fig. 1). The area is part of the Basin and Range Province, which is characterized by isolated mountain ranges rising abruptly from broad, alluvium-filled basins. Rocks within the study area are variable in lithology and age, but most outcrops are composed of Mesozoic plutonic rocks, which are the focus of this research. The climate of the region is arid, with hot and dry summers and warm and less dry winters. Precipitation is typically scarce and spotty, and varies from 110 to 150 mm yr^{-1}, mostly associated with winter Pacific frontal storms. The major vegetation types in the upland watersheds are the Mojave creosotebush scrub and the blackbrush scrub, which are dominated by creosotebush (*Larrea tridenta*), white bursage (*Ambrosia dumosa*), and blackbrush (*Coleogyne ramosissima*) (Fahnestock and Novak-Echenique, 2000).

The soils on upland watersheds are developed in residuum and colluvium from plutonic rocks and are well drained with coarse sandy loam to loam texture, and classified as loamy-skeletal, mixed, superactive, calcareous, thermic Lithic Torriorthents and loamy-skeletal, mixed, mesic Lithic Haplargids (Fahnestock and Novak-Echenique, 2000). The soils exhibit high spatial variability in thickness that range from 20 cm to 150 cm (Crouvi et al., 2013). This variability is evident mostly in moderate to steep slopes ($\sim > 15^{\circ}$), in which extreme heterogeneity in soil thickness and texture exists; In the upper and middle parts of these slopes, piles of boulders occur adjacent to areas covered with coarse to very coarse gravels (2–5 cm), which in turn cover soil up to 1 m thick. The stages of carbonate morphology of the soils vary and range from stage I (undeveloped calcic soil) to stage IV (well-developed calcic soil with an indurated petrocalcic horizon) (Crouvi et al., 2013). The content of aeolian, external sediments in the upland soils is estimated to be high, ranging from 50 to 100 % of the profiles

ESURFD
2, 535–574, 2014

considering only the fine fraction of the soil (< 2 mm), but only 11 to 33 % of the total soil thickness (including gravels).

Previous estimations of soil erosion rates in the Mojave Desert focused on watershed-scale long-term (millennial) erosion rates on granite uplands and alluvial-fan deposits (Nichols et al., 2002, 2007) and decadal-scale erosion rates on alluvial-fan deposits (Griffiths et al., 2006). To the best of our knowledge, there is no published estimation of upland hillslope soil erosion rates in the Mojave Desert over any time scale. As such, this study fills an important knowledge gap.

2.2 Sampling

We chose four study sites in the study area (Figs. 1 and 2). All sites are composed of plutonic rocks: two sites are composed of granite, one site of quartz-monzonite (i.e., a quartz-poor granite), and one site of diorite (Table 1). The latter was selected in order to examine erosion rates in an intermediate igneous lithology, composed primarily of less weathering-resistant minerals (i.e., plagioclase feldspar). Slope gradient varies among the sites, and ranges from average slope of 5 to 25°. Samples for ^{137}Cs analysis were collected during June 2011 along transects on NE- or NW-trending slopes for each site; additional SW-trending downslope transects were sampled for two of the sites (EPR3 and BRH). We sampled soil profiles for ^{137}Cs concentration along the transects in four topographic positions: summit, shoulder, backslope and footslope (toeslope was not sampled) (Birkeland, 1999) (note that for one site, GM2, the summit is not the highest point in the area, but it is the highest point for the relevant transect). Sample intervals were 20 to 40 m between topographic positions (Figs. 2 and 3). At each topographic position we dug and sampled two shallow soil profiles, separated by 1–5 m. Thus, a total of eight different soil profiles were sampled for each transect (beside one site, EPR3, in which one summit position was used for both transects). Soil was sampled using a small shovel at 3 cm intervals, reaching a maximum depth of 9 cm. The total number of soil profiles and ^{137}Cs samples analyzed in this study is 46 and 138, respectively.

ESURFD
2, 535–574, 2014

The eight soil profiles located on the summits were chosen to be used for a reference for un-disturbed sites. We assumed that in these locations sediment (fluvial) deposition and erosion are minimal. Yet, out of eight potential soil profiles we eventually used only two, one at site EPR2 and one at GM2, for the calculation of the reference site, based on their high total inventory and on their depth distributions of ^{137}Cs that exhibit peak concentrations at the surface and exponentially decline with depth, as expected from un-disturbed depth profiles (Fig. 3a and b) (Chappell, 1999). The other six profiles, although located on summits, exhibit eroded depth profile of ^{137}Cs. The average total ^{137}Cs inventory of the two un-eroded summit profiles was used as a reference value for all four study sites.

To investigate soil development along the sampled transects we dug 5–6 additional deep soil pits per transect (Fig. 2) using a hand shovel and a trencher. The soil pits were dug down to the depth of unweathered bedrock (R horizon) defined as the "depth to refusal", the contact where soil can no longer be excavated by hand, hydraulic core, or drill (Soil Survey Staff, 1999). The soils were described and sampled following standard methods (Soil Survey Staff, 1999). At each soil pit location in two of the sites, the rock coverage percentage was estimated by counting the number of rocks > 0.5 m in a 1 m interval along 50 m transect laid along the topographic contours (these transects were used by Crouvi et al. (2013) to estimate presence/absence of soil). The rock coverage for the other two less-rocky sites was estimated visually. Vegetation coverage was estimated for the area immediately surrounding of each soil profile. We analyzed two profiles per transect for particle size distribution (PSD), electrical conductivity (EC), and pH analyses: one at the summit and one at the footslope (except for one site for which only one profile at the summit was analyzed). Samples were collected from genetic horizons which were brought back to the laboratory, air-dried, sieved with a 2 mm sieve and split. Analysis of PSD was carried out using a Beckman Coulter LS 13 320 laser diffraction particle size analyzer, following the procedure described in Crouvi et al. (2013). Organic matter was removed from the soil samples using NaOCl before the PSD analysis. Saturated soil pastes were extracted with the procedure outlined in Soil Survey Laboratory

ESURFD
2, 535–574, 2014

Staff (1999) and EC and pH were determined on saturation extracts immediately after extraction.

2.3 Analysis of ^{137}Cs in soil samples

Soil samples were dried and sieved through a 2 mm screen to break aggregates and homogenize the sample. The content of rock fragments (> 2 mm) in each soil profile was used as a proxy for the relative presence of rock exposed upslope of the location of the soil profile (Nearing et al., 2005). The samples (< 2 mm) were weighed, placed into 120 mL tin cans in a uniform layer and sealed with air-tight lid. The depth of the samples in the cans was measured in order to calculate sample density. The analysis for ^{137}Cs was performed using gamma ray spectrometry system consisting of two n-type high-purity closed-end coaxial germanium detectors (Canberra GC4019) with > 30 % relative efficiency coupled with an amplifier and a multi-channel analyzer (DSA-2000A). The detectors were shielded with 100 mm thick layer of lead. The system was calibrated using mixed radionuclide reference material IAEA-327 (Dekner, 1996) obtained from International Atomic Energy Agency. The gamma emission spectrum was obtained over 0–2 MeV range with the resolution of 0.24 keV (8192 channels). Measurement and spectrum analysis was conducted using Genie-2000 Spectroscopy software (Canberra, 2009). The samples were counted for at least 80 000 s. Activity of ^{137}Cs (mBq g^{-1}) was calculated from 661.6 keV photopeak. The analysis included correction factor for self-attenuation due to variation of sample volume and density (Quindos et al., 2006). To convert the ^{137}Cs activities (mBq g^{-1}) to ^{137}Cs inventories (Bq m^{-2}) we used a uniform bulk density of 1.25 g cm^{-3}. This value was estimated from the analyses of 7 soil samples taken from B horizon of the studied soils at the study sites (for more details see Crouvi et al., 2013).

ESURFD
2, 535–574, 2014

2.4 Estimation of erosion and deposition rates

A profile distribution model was utilized to convert measured ^{137}Cs inventories into soil erosion and deposition rates on the studied slopes (Walling and He, 1999). The model assumes that total ^{137}Cs fallout occurred in 1963 (fallout peak) and in the absence of cultivation, the nuclide is concentrated near the surface while its depth distribution exhibits exponential decline (Walling and He, 1999):

$$A'(x) = A_{\text{ref}}(1 - e^{-x/h_0}) \quad (1)$$

where $A'(x)$ is the ^{137}Cs inventory (Bq m^{-2}) above cumulative mass depth x (kg m^{-2}), A_{ref} is the ^{137}Cs total inventory at an undisturbed reference site (Bq m^{-2}), and h_0 (kg m^{-2}) is profile shape coefficient determined experimentally from the reference site depth profile.

Rate of soil erosion and deposition Y (t ha^{-1} yr^{-1}), was determined by comparing measured inventory to the reference ^{137}Cs inventory as follows (Walling and He, 1999):

$$Y = \frac{10}{t - 1963} \ln\left(\frac{1 - x}{100}\right) h_0 \quad (2)$$

where t (yr) is the year of sample collection, and x (%) is the reduction in total ^{137}Cs inventory compared to the reference inventory. Note that negative values of Y are net erosion whereas positive values are net deposition. Average erosion/deposition rates were calculated for each pair of adjacent soil profiles per topographic position.

2.5 Estimating the topographical factors at sampling sites

We used a 1 m pixel digital elevation model (DEM) bare-earth dataset derived from LIDAR to compute slope gradients and curvature values. Prior to calculating the slope and curvature of the topography, we smoothed the DEM at a spatial scale of 5 m, which contains significant small-scale variability due to animal burrows, shrubs, etc.

ESURFD
2, 535–574, 2014

This smoothing procedure greatly reduces the small-scale variability in the DEM without significantly affecting the shape of the landscape at the hillslope scale (Pelletier and Rasmussen, 2009; Pelletier et al., 2011). For each ^{137}Cs sampling location we extracted the slope gradient and curvature value from the analysis. A positive curvature indicates that the surface is concave at that cell whereas a negative curvature indicates that the surface is convex at that cell. A value of zero indicates that the surface at the sampling point is planar. We calculated the Laplacian curvature using four nearest neighbors (i.e., the curvature in both directions of steepest decent and along-contour). As curvature values calculated from DEM are known to depend on the gird size (e.g., Heimsath et al., 1999) we examined a 5 m curvature map, in addition to the 1 m values. According to Heimsath et al. (1999), curvature generally becomes scale independent over 5 m grid size since most pit and mound topography occurs at spatial scales less than 5 m. We also calculated a topographic proxy for shear stress by overland flow by multiplying the slope gradient by the square root of the contributing area (contributing area was calculated following the multiple flow direction algorithm of Freeman, 1991).

3 Results

3.1 ^{137}Cs inventories

The ^{137}Cs mass activities and inventories in the soil samples varied greatly and for all depth increments (n = 138) ranged between 0 and 16.04 mBq g^{-1}, and between 0 and 601.4 Bq m^{-2}, respectively (see Supplement data). The average ^{137}Cs inventory of the reference sites is 834 (±67) Bq m^{-2}, with a coefficient variation (CV) of 8 % (Table 2).

In general, site GM2 exhibits the highest mean ^{137}Cs inventory of all study sites; site EPR2 exhibits lower mean value with lower minimal and maximal values (Table 2). The two other sites, EPR3 and BRH, exhibit much lower mean values of ^{137}Cs inventory with few soil profiles in which no ^{137}Cs was detected (two profiles at EPR3 and five at BRH). The ^{137}Cs depth profiles and total inventories on hillslopes vary within and

ESURFD
2, 535–574, 2014

between study sites (Figs. 2 and 3). Differences in ^{137}Cs inventories between sampling pairs (located 1–5 m apart) vary significantly (Fig. 4) – whereas half of the pairs shows relatively low difference (< 100 Bq m^{-2}), the other half exhibits large differences that range from 100 to 680 Bq m^{-2}. At site GM2, all soil profile pairs show similar inventories per topographic position besides the summit. Generally, the ^{137}Cs inventories increase downslope. Most depth profiles exhibit detectable ^{137}Cs even at the lower sampling interval (6–9 cm) (see insets in Fig. 3a). Some depth profiles are exponential whereas others decrease from high surficial activities to steady activities at depths of 3–9 cm. At site EPR2 the two summit soil profiles show similar, high inventories; shoulder and backslope positions exhibit low inventories, whereas the footslope position reveals intermediate values (Fig. 3b). For half of the soil profiles ^{137}Cs activities were detected only at the upper most sampling interval (0–3 cm) whereas for the rest ^{137}Cs activities occur also at depth of 3–6 cm, with zero to negligible activities at depth of 6–9 cm. Similar to site EPR2, site EPR3 exhibits variability of ^{137}Cs inventories per topographic position for part of the profiles (Fig. 3c). Two of the profiles out of the fourteen studied revealed no detectable ^{137}Cs activities at all, whereas for seven profiles ^{137}Cs was detected only at depth of 0–3 cm. Three profiles revealed detectable ^{137}Cs at the depth of 3–6 cm; two profiles exhibit no detectable ^{137}Cs at the surface and negligible activities at lower depths that suggest loss of ^{137}Cs layer with subsequent deposition or other perturbation. At site BRH the ^{137}Cs inventories vary among topographic positions (Fig. 3d and e). Depth profiles are different than other sites and follow the low inventories found for this site: in five profiles out of the sixteen studied no ^{137}Cs was detected at all; for seven profiles ^{137}Cs was detected only at the surface. Only at four profiles ^{137}Cs was detected at depth of 3–6 cm.

3.2 Calculated erosion rates and their spatial patterns

Soil erosion rates vary among the sites, following differences in ^{137}Cs inventories (Fig. 5; Table 3). Site GM2 exhibits the lowest mean erosion rate among all sites

ESURFD
2, 535–574, 2014

($-3.60\,t\,ha^{-1}\,yr^{-1}$), followed by site EPR2 ($-8.06\,t\,ha^{-1}\,yr^{-1}$). The two other sites, EPR3 and BRH, exhibit higher mean erosion rates (-17.90 and $-24.34\,t\,ha^{-1}\,yr^{-1}$, respectively) partly because they include soil profiles that lack detectable ^{137}Cs inventories.

Soil erosion rates vary also on hillslopes (Figs. 5 and 6). Site GM2 exhibits two contradicting erosion rates at the summit position, with an average rate of $-5.3 \pm 8.1\,t\,ha^{-1}\,yr^{-1}$. The two mid-slope locations show uniform and slightly lower rates, whereas the base of the slope shows almost zero erosion rate. Site EPR2 shows uniform and minimal erosion rate at the summit (average of $-0.8 \pm 0.5\,t\,ha^{-1}\,yr^{-1}$) and much higher rates at mid-slope locations (average values around $-12\,t\,ha^{-1}\,yr^{-1}$). Although erosion rate decreases at the base of the slope it is still low to intermediate (average $-7.4 \pm 3.8\,t\,ha^{-1}\,yr^{-1}$). Site EPR3 exhibits higher erosion rates than the above mentioned sites. At this site one of the summit profiles lacks any detectable ^{137}Cs, making the erosion rate for this location at least $-51.9\,t\,ha^{-1}\,yr^{-1}$; the adjacent profile also shows high erosion rate ($-23.8\,t\,ha^{-1}\,yr^{-1}$), yielding an average erosion rate at the summit of $-37.8 \pm 19.9\,t\,ha^{-1}\,yr^{-1}$. The NE slope exhibits gradual decrease in average erosion rates downslope from -12.4 ± 10.9 to $-10.5 \pm 2.2\,t\,ha^{-1}\,yr^{-1}$, reaching $-6.8 \pm 2.0\,t\,ha^{-1}\,yr^{-1}$ at the base of the slope. The SW slope exhibits higher erosion rates with average rate of $\sim -13\,t\,ha^{-1}\,yr^{-1}$ at mid slope positions. The base of the slope exhibits high erosion rate (average of $-31.8 \pm 28.3\,t\,ha^{-1}\,yr^{-1}$). Site BRH includes soil profiles with no detectable ^{137}Cs that are located in all topographic locations, including the summit. For these locations the average erosion rate is $-31\,t\,ha^{-1}\,yr^{-1}$. The rest of the profiles exhibit low to intermediate erosion rates (average rates from -6 to $-14\,t\,ha^{-1}\,yr^{-1}$).

3.3 Effects of topographic factors and rock fragments on soil erosion rate

Site GM2 exhibits the steepest topographic slopes at the sampling soil pits, ranging from 14 to 29° ; slopes at site EPR2 range from 6 to 18°, at site EPR3 from 5 to 15°, and at site BRH from 2 to 12° (Fig. 7a). Average negative curvature is the

ESURFD
2, 535–574, 2014

highest at site GM2 ($0.011 \pm 0.025\,m^{-1}$), followed by site EPR2 ($0.009 \pm 0.018\,m^{-1}$), site BRH ($0.007 \pm 0.006\,m^{-1}$), and site EPR3 ($0.005 \pm 0.010\,m^{-1}$) (Fig. 7b). Values of slope × sqrt(contributing area) are mostly < 1.7 m; only for few locations in site GM2 were values of 3 to 4 m observed (Fig. 7c). For each study site we found no significant relationship between soil erosion rates and topographic slope, between erosion rates and topographic curvature (both 1 m and 5 m), and between erosion rates and slope × sqrt(contributing area) (In this procedure we did not account for the profiles with no detectable ^{137}Cs inventories that yield high and only minimal erosion rates.)

Yet, as our sampling population per study site is relatively low (8 to 12 values), an alternative approach is to examine these relationships for all four study sites together, treating them as one sampling population. Doing so, we found a negative significant relationship between soil erosion and topographic slope (i.e., steeper slopes correlated to lesser erosion) ($n = 39$; $r^2 = 0.11$; $p = 0.04$) (Fig. 7a). Moreover, when we perform this regression without the data of site EPR2 that is composed of different (diorite) lithology, the relationship is even stronger ($n = 31$; $r^2 = 0.22$; $p = 0.008$). Similar negative significant relationships were observed between soil erosion and slope × sqrt (contributing area) ($n = 39$; $r^2 = 0.14$; $p = 0.02$ for all data; $n = 31$; $r^2 = 0.24$; $p = 0.005$ for all data except for EPR2) (Fig. 7c). On the other hand, regressing the topographic curvature data (both 1 and 5 m) of all sites (with or without the dioritic site) against soil erosion rates reveals no linear relationship between these variables (Fig. 7b).

The mean value of volume fraction of rocks in the soil profile (0–9 cm) at site GM2 is 46.6 %, much higher than the other study sites (Table 4). Sites EPR2 and EPR3 show lower and similar average percentages (26.3 and 28.5 %, respectively), and BRH exhibits the lowest average rock fragments percentage (20.6 %). We found no significant relationship between soil erosion rates and percent of rock fragments in soil profiles within each study site, however, when we examined all study sites as one population we found a significant negative linear relationship ($r^2 = 0.26$; $p = 0.0008$) (Fig. 7d). As for the slope data, the relationship is even stronger ($r^2 = 0.38$; $p = 0.0002$) when we do not account for the dioritic site.

ESURFD
2, 535–574, 2014

3.4 Soil catena characteristics

Site GM2 is characterized by the highest rock and vegetation coverage of all studied sites (33 and 52 %, respectively) (Table 1). Most soils have A/Bk/Ck/R or A/Bk/BkC/R profiles; the backslope soil has a A/Bk/R profile. Soil thickness is relatively constant (40–50 cm), without a clear downslope trend along the 130 m catenary length (Fig. 6a); the backslope profile is an exception, with a 85 cm thick soil. The thickness of A horizon (and thus the depth to top of Bk horizon) is relatively constant and ranges from 7 to 12 cm (except for at the backslope profile). Soil texture of A and Bk horizons changes from sandy-loam at the summit to loamy-sand at the footslope (Fig. 8). EC values for soil horizons at the summit are between 70–100 $\mu S\,cm^{-1}$ whereas at the footslope they are higher and range from 200 to 400 $\mu S\,cm^{-1}$ (Fig. 6a). In terms of carbonate morphology, the carbonate stage of the soils is mostly II, with slightly more developed soils (II–III) at the lower part of the slope.

Site EPR2 is characterized by slightly lower rock and vegetation coverage than site GM2 (27 and 39 %, respectively) (Table 1). Similar to site GM2, soils have either A/Bk/Ck/R or A/Bk/BkC/R profiles. Soil thickness slightly increases downslope along the 130 m catenary length from ~ 50 to ~ 70 cm (Fig. 6b) (see also Crouvi et al., 2013). A horizon is thin and constant in thickness along the transect (3 cm in five profiles out of the six studied). Thickness and texture of Bk horizon change downslope: at the summit it is 14 cm thick and of loamy-sand to sandy-loam texture whereas at the footslope it is 31 cm thick and of sandy-loam texture (Figs. 6b and 8). Similar to site GM2, also at site EPR2 the footslope profile horizons accumulated more salts than the summit (25–600 vs. 2–300 $\mu S\,cm^{-1}$, respectively) (Fig. 6b).The soils are relatively cobble and stone-poor (10–30 % in the A and B horizons) (Crouvi et al., 2013) and are not well-developed in terms of carbonate morphology, with carbonate stages of I–II along the transect without a clear trend in soil development downslope.

Site EPR3 is characterized by absence of large (> 0.5 m) surficial rocks, and a relatively low vegetation coverage (20 %). The soils at this site are more heterogeneous

ESURFD
2, 535–574, 2014

than the previously described sites. The summit soil has a A/Btk/R profile; the soils along the SSW transect have A/Bk/R or A/Bk/Ck/R profiles. Soil thickness gradually increases downslope along the 85 m catenary length from 34 cm at the summit to 77–150 cm at the lower parts of the slope (Fig. 6c) (see also Crouvi et al., 2013). Depth to top of Bk horizon also increases from ∼ 2 cm at the upper parts of the slopes to 40–50 cm at the bottom. The texture of the Btk horizon changes from sandy-loam at the summit to clay loam at the base (Fig. 8). Cobble and stone percentages range from 30 to 80 % in A and B horizons (see also Crouvi et al., 2013). EC values for soil horizons are higher than previous sites (50–1000 $\mu S\,cm^{-1}$) whereas the summit profile exhibit higher EC values than the footslope (Fig. 6c). The soils show an increasing trend in soil development with carbonate morphologic stages of mostly I at the upper parts of the slope, to stage II and III at the lower parts. Most of the soils along the opposite and gentle sloping NNE transect have a pronounced Bt horizon. Soil thickness changes from 25 to 80 cm without a clear trend downslope (Fig. 6c); fluvial deposits were observed at the base of the footslope profile. Depth to top of Bk (or Btk) horizon (18–35 cm) and carbonate morphologic stage (I to II) vary without a clear downslope trend. No PSD data are available for this transect.

Site BRH is characterized by gentle slopes and great variation in soil thickness from ∼ 0.2 m on the flat summits to 1–1.7 m further downslope (Crouvi et al., 2013). The northward transect exhibit soils with a pronounced C horizon with A/AB/Rck, A/Bgr/CBkm, and A/Bgr/Bkm/Ck profiles (Fig. 6d). The soils along the southwest transect have A/Bkm/Rk profile at the summit, and A/Bkm/Bk/Rk profile at the backslope. The footslope profile is similar to the backslope one, but fluvial sediments were found at the base of the pit (Fig. 6e). In both transects soil thickness increases downslope and A horizon is relatively thick (15–30 cm) without signs of carbonate accumulation. In most soils A horizon abruptly overlay hard petrocalcic horizon (Bkm) that represents the greatest degree of carbonate morphology development found in this study (stages III–IV). At the summit, soil texture of A horizon is finer than the other sites (clay-loam, loam to silt-loam), and resemble the texture of pure aeolian sediments that were sampled on

ESURFD
2, 535–574, 2014

a nearby basalt plateau (Crouvi et al., 2013) (Fig. 8). At this site EC values for the summit profile horizons are the highest measured in this study and range from 1000 to 4000 $\mu S\,cm^{-1}$.

4 Discussion

Our study provides a detailed estimation on the distribution of ^{137}Cs inventories and decadal-scale slope wash erosion rates along 6 transects in 4 study sites in the Mojave Desert. The most striking observation is that ^{137}Cs inventories (and subsequently soil erosion rates) vary at all spatial scales: at 1–5 m (in-between sampling pairs), at 20–40 m (on hillslopes) and at 5–30 km (between study sites). The variability in erosion rates at a meter scale suggests that even for the same topographic position there is large variation in runoff generation and flow continuity at least for part of the examined profiles, as often occurs in deserts (e.g., Yair and Kossovsky, 2002). This is also emphasized by the great spatial variability in soil thickness in the study sites, reported to occur at a meter scale (Crouvi et al., 2013) (and see also below). The variability in erosion rates at all scales affected our selection of the soil profiles to be used as reference sites, which is one of the most important steps in estimating erosion rates using ^{137}Cs fallout (Parsons and Foster, 2011; Mabit et al., 2013). Here we used only two summit profiles out of potential eight profiles for the calculation of the average reference site. The average reference inventory ($834 \pm 67\,Bq\,m^{-2}$) is in general agreement with the theoretical inventory for Ft. Irwin, calculated using global ^{137}Cs distribution model (Walling and He, 2000). This model is designed to estimate likely total inventory for a specific location taking into account longitudinal and latitudinal variation in fallout input, secondary inputs (Chernobyl accident), precipitation patterns, and nuclide decay. According to the global model, the reference ^{137}Cs inventory is $949\,Bq\,m^{-2}$, only 13 % difference from our field-based reference site. In addition, the precision of the reference site used here is not expected to affect our understanding on the controls on slope wash erosion, as all calculated erosion rates will be offset in a similar way.

ESURFD
2, 535–574, 2014

Despite the large variability in erosion rates at this scale, averaging the rates per study site revealed that the mean soil erosion rate is controlled mostly by rock and vegetation coverage (Tables 1 and 3): sites with higher coverage of rock and vegetation exhibit lower soil erosion rates compared to sites with mostly bare soil. Slope gradients also differ between sites, but these differences should cause greater erosion rates at the steeper sites, rather than less as was observed (in case surface cover was held constant). Since the slopes get rockier as they get steeper (Table 1) (Abrahams et al., 1985; Hirmas et al., 2011), the increase in erosion rates with increasing slope is of lesser importance than the inhibiting effect of greater rock cover (which increases with increasing slope), as found in semi-arid regions (Nearing et al., 1999, 2005)

To better understand the soil erosion rates within sites (on hillslopes), we used regression analyses of individual rates with the potential factors that affect soil erosion, but found that none was significant, probably due to the low number of points per site (8–12) (for example, Nearing, 2005 used > 60 sampling points to show correlations within sites). As three of the four studied sites are of similar lithology (granite and quartz monzonite), we grouped them as one sampling population ($n = 31$). We also examined the regressions for all data points with the addition of the dioritic site ($n = 39$). The results of these regressions indicate that soil erosion rate is not correlated with topographic curvature, is negatively correlated with topographic slope, and negatively correlated with rock fragments in soil profile. The latter implies that as rock fragments increase in soil profile, soil erosion rate decreases and suggests that soil erosion rate is governed by the distribution of upslope surficial rocks. The negative correlation between slope and soil erosion rate is the opposite of what we expected. We think that this correlation simply represents the fact that steeper slopes generally exhibit higher percentage of rock fragment in soil profiles (Tables 1 and 4). Thus, steep slopes with abundant surficial rocks exhibit lower erosion rates than mild slopes with limited abundance of rock fragments (Yair and Klein, 1973; Hirmas et al., 2011). The explanation for the positive correlation between slope and rock coverage has been attributed to past erosion – steeper slopes are believed to have undergone greater erosion in the

ESURFD
2, 535–574, 2014

past that removed fine material and increased the rock cover. Subsequently, increase in rock cover led to reduce in soil erosion rate, resulting in a relatively uniform erosion rates across the hillslope (a state of slope-velocity equilibrium) (e.g., Govers et al., 2006). Thus, the control of rock coverage on erosion rates shown here, together with the apparent independence of direct control of slope gradient over erosion rates, are best explained in terms of hydraulic controls by the rocks and initial conditions of the sites and the associated slope-velocity equilibrium the develops on slopes (Nearing et al., 1999, 2005).

Our interpretation that higher rock and vegetation coverage decreases slope-wash–driven soil erosion rates is in agreement with previous studies that were done in more humid climates (Poesen et al., 1994; Riebe et al., 2000; Cerda, 2001; Granger et al., 2001; Nearing et al., 2005). Yet, studies from a different arid region (Israel) (Yair and Enzel, 1987; Yair, 1990) found a positive relationship between rock coverage and soil erosion by water, the opposite from our findings. The reason for this discrepancy is most likely related to difference in lithology and subsequently in surficial rock size and position in the soil (see Fig. 7 in Poesen et al., 1994). The hillslopes studied here exhibit negative relationship between rock coverage and erosion rates as (1) most of the plutonic rocks are not well embedded in the soil, creating large spaces in-between boulders and cracks that favors high infiltration rate, and (2) the topsoil texture is mostly sandy-loam, with 60–75 % sand (Fig. 8) that originate from the in-situ weathering of the rocks and from aeolian input from adjacent sand-rich channels, promoting infiltration and depressing runoff as compared to surfaces with a silt-rich crust (e.g., Kidron et al., 2012). On the other hand, a positive relationship between rock coverage and erosion rates occurs in the Negev Desert where (1) the carbonate bedrock is usually well-embedded in the soil, and (2) the soil is composed mostly of pure silt-sized dust particles with loamy texture. In summary, although both regions exhibit similar rainfall characteristics (e.g., mean annual precipitation of 100–150 mm), the difference in lithology governs the differences in the position of the surficial rocks and in soil texture that affect infiltration and runoff, and in turn yield different soil erosion rates.

ESURFD
2, 535–574, 2014

The spatial variability and absolute values of erosion rates is mirrored in the soil catena data within and between study sites. At site GM2, the relatively constant total soil thickness and depth to top Bk horizon, the presence of weathered C horizon, and the limited amount of soluble slats in the profiles suggest that (1) water infiltration is an important process along the slope, and (2) slope wash erosion is relatively constant and limited. These interpretations are in agreement with our findings of low and relatively constant erosion rates. At the dioritic site (EPR2) soil characteristics do not change dramatically downlslope and are in agreement with the relatively constant and intermediate erosion rates. Soils profiles in EPR3 are diverse in terms of profile horizonation, depth to top Bk horizon and thickness. Most profiles lack the C and Bk horizons and exhibit more clay-rich B horizons (Bt) that directly overlay the un-weathered bedrock (R horizon), suggesting limited infiltration and high erosion rates. This is in agreement with the relatively high soluble slats content. Only few soils exhibit a clear C horizon underlying Bk horizon, suggesting high infiltration rate and low runoff. Overall, the soil data suggest high and varied erosion rates along the hillslopes, with different amounts of water infiltrating the soils, in agreement with the Cesium-137 results. At site BRH, most profiles presents buried soil, with a well-developed calcic horizon (Bkm horizon; carbonate stages II–IV) (see also Crouvi et al., 2013). These profiles are abruptly overlain by a soil profile composed mostly by a 15–30 cm thick A horizon. Lack of recent accumulation of pedogenic carbonate in the upper 30 cm of the soils (as opposed to what was found in the other studied sites), together with the high amount of soluble salts suggest that limited amount of water infiltrate the soil. This in turn suggests high runoff coefficient and high erosion rates for this site, as found by using the ^{137}Cs inventories. In addition, this site exhibit loamy texture for the A and A/Bgr horizons that promotes runoff and erosion.

Our study also contributes to the relative importance of different soil erosion processes in deserts, namely soil erosion by water (slope wash) vs. colluvial soil erosion (we assume that soil erosion by wind is negligible here due to the crusted topsoil in all sites). Erosion rates estimated here (and in other studies that use ^{137}Cs inventories)

ESURFD
2, 535–574, 2014

are most likely related only to slope wash. This is based on the fact that soil erosion rates estimated using ^{137}Cs inventories represent ~ 50 years of erosion; this time period does not capture the slower downslope movement of soil due to creep and bioturbation (i.e., colluvial erosion in slopes not subject to landsliding). In the case of soil erosion by water, we do not expect to find a significant linear relationship between topographic curvature and erosion rate, whereas this relationship is significant when diffusive processes dominate (e.g., Heimsath et al., 2005; Roering, 2008; Pelletier and Rasmussen, 2009). In our study we did not find a significant linear relationship between soil erosion rate (by water) and curvature (Fig. 7b) (see also Nearing et al., 2005); However, examination of Fig. 7b reveals that the data points form the shape of an inverted isosceles triangle that limits the maximal erosion rates. The lower vertex of the triangle is located at a slightly convex curvature (negative curvature of ~ $-0.012\,m^{-1}$) and maximal erosion rates decrease as curvature tends to be both more convex and concave. This is expected, as in highly convex locations erosion is governed by colluvial transport and thus rates of soil erosion by water decrease as the surface is more convex; in highly concave locations rates of soil erosion by water decrease as sediments tends to be deposited rather than eroded in concave dominated areas. In more humid regions, studies report similar, but not identical, relationships. Kaste et al. (2006) showed that convex sites have significantly higher ^{137}Cs soil inventories than sites that are flat or concave and concluded that slope wash erosion at their study site is focused in convergent areas, whereas convex landforms have remained stable. O'Farrell et al. (2007) found a positive linear correlation between ^{137}Cs inventories and topographic curvature at convex sites and concluded that these sites are governed by diffusion-like erosion. On the other hand, at concave sites the authors found that overland flow is the dominant erosion process.

Our findings suggest that in the Mojave Desert, current rates of soil erosion by slope wash are higher along gentle sloping and relatively bare slopes compared to steep and rocky slopes. Our results strengthen previous studies that showed evidence for slope wash along slopes up to 24° in the Mojave (Abrahams et al., 1984). We caution that it is

ESURFD
2, 535–574, 2014

difficult to make inferences about the processes or rates of landscape denudation over geologic time scales from this study given the short time scale captured by the ^{137}Cs method together with the fact that ^{137}Cs binds preferentially to fine particles. A large fraction of the fine material in these soils is sourced by aeolian dust (Crouvi et al., 2013), and hence the removal of these particles does not necessarily result in landscape denudation because some of the fine particles removed from hillslopes are transported to nearby playas (i.e., Bicycle Lake Playa) and where they are available for aeolian transport and redeposition in a continuous cycle. Despite the differences in time scales, our findings are consistent with the fact that Crouvi et al. (2013) found a relatively poor fit between their model predictions (based on an assumption of colluvial transport only) and observed soil thicknesses for the BRH site, while they found a relatively good fit at a steep, rocky site (EPR2) where slope wash erosion was likely low according to the results presented here.

The average soil erosion rates found here (range from −3.6 to −24.3 t ha^{-1} yr^{-1} per site) are higher than rates found in semi-arid regions, such as southeastern Arizona (mean −3.2 and −5.6 t ha^{-1} yr^{-1} for two studied sites, individual rates < 10 t ha^{-1} yr^{-1}) (Nearing et al., 2005). As the value range of rock fragments in soil is similar in both studied sites (Mojave and Sonoran deserts) and range from 10 to 55 %, the probable cause for this discrepancy is vegetation, which is more abundant in semi-arid regions than arid areas. Hillslopes with low coverage of large rock fragments and vegetation, but with high concentration of fines (i.e., dust deposits) are relatively abundant in the Mojave Desert (i.e., sites EPR3 and BRH). Thus, along certain hillslopes, arid regions can exhibit higher erosion rates compared to the wetter semi-arid regions (see also Douglas, 1967).

The average soil erosion rates found in this study are also higher than previous estimations of soil erosion rates at the watershed scale for the Mojave Desert. Nichols et al. (2002) studied long-term (millennial) soil erosion rates of 6–8 km^2 drainage basins on Mesozoic granitic rocks, about 180 km southeast of the current study site, in an area that is currently more arid than Ft. Irwin (mean annual precipitation of 79 mm). Based

ESURFD
2, 535–574, 2014

on analyses of cosmogenic nuclides in alluvial sediment samples, Nichols et al. (2002) estimated the long-term average sediment generation rate to be 0.91–1.04 t ha^{-1} yr^{-1} (see Table 3 in Nichols et al., 2002). The discrepancy of more than one order of magnitude between these estimations and our findings is best explained by the spatial scale differences and by the high storage capacity of the fluvial systems in the Mojave Desert. Although erosion rates are higher on hillslopes, most of the eroded material is stored at the adjacent foothills or small valleys that drain the slopes, whereas only limited material reaches farther away and is deposited in the piedmonts. Two additional studies that estimated soil erosion rates in the Mojave Desert focused on alluvial fans and both found very low rates: Nichols et al. (2007) used cosmogenic nuclides to estimate soil erosion rate of ~ -0.36 t ha^{-1} yr^{-1} for a low-relief Tertiary alluvial fan deposits located in Ft. Irwin, only few km from site GM2 (Fig. 1). Similar low soil erosion rates were estimated by Griffiths et al. (2006) who studied sediment yield of small drainage basins (< 1 km^2) on alluvial fans located 50–200 km east, northeast and north of Ft. Irwin. Using ^{137}Cs inventories Griffiths et al. (2006) found that soil erosion rate ranged from -0.09 to -0.48 t ha^{-1} yr^{-1}. The low soil erosion rates of fan deposits reported by these two studies are best explained by the great infiltration capacity and low runoff yield of the sediments that are mostly covered with gravels and clasts, combined together with gentle slopes. We should note that when comparing erosion rates based on ^{137}Cs inventories with rates estimated using cosmogenic nuclides, part of the discrepancy between the rates can be explained by ^{137}Cs dust influx. As we assume that no erosion occurred at the reference sites, these sites have potentially accumulated ^{137}Cs-enriched dust. Areas downslope with low ^{137}Cs inventories might be eroding fast enough to negate dust accumulation, and thus their net erosion rate should be smaller. Yet, as previous estimations on Holocene dust accumulation rates in the Mojave are about 0.088 t ha^{-1} yr^{-1} (Reheis et al., 1995; Crouvi et al., 2013), this process can explain an overestimation of erosion rates up to 4.4 t ha^{-1} yr^{-1}, and thus storage capacity is probably still the best explanation of the difference between millennial to decadal rates.

ESURFD
2, 535–574, 2014

5 Summary

The results of this study show that in the Mojave Desert, rates of soil erosion by water along hillslopes are mainly controlled by surficial rock coverage, similar to findings from semi-arid regions (e.g., Sonoran Desert). Steep slopes are characterize by higher rock and vegetation coverage and exhibit lower soil erosion rates compared to gentle slopes that are characterized by mostly bare soil. As the slopes get rockier as they get steeper, the increase in soil erosion rates with greater slope is of lesser significance than the hindering effect of higher rock coverage. The abundance of large plutonic rock fragments on steep slopes that are not well embedded in the soil creates large spaces in-between boulders and cracks that favors high infiltration rate. This, together with sandy-loam topsoil texture hinders runoff and erosion. Gentle slopes exhibit higher erosion rates that are even higher than rates observed in semi-arid regions, probably due to the lower rock and vegetation coverage in the studied slopes, together with the loamy soil texture. Overall the observed decadal erosion rates on the hillslope scale are higher than previous estimations of millennial erosion rates for the Mojave, estimated for the watershed scale. This discrepancy is best explained by the spatial scale differences.

The Supplement related to this article is available online at doi:10.5194/esurfd-2-535-2014-supplement.

Acknowledgements. We thank Ruth Sparks and Dave Housman from ITAM, Ft. Irwin, for helping with the logistics and permits for the field trips. We thank Mercer Meding, Justine Peal Mayo, Natalie Lucas, Chris Clingensmith and Stephanie Castro for helping with the laboratory analyses. We wish to thank Aaron Yair from the Hebrew University for reviewing an early draft of this manuscript. This study was funded by the Terrestrial Sciences Program of the Army Research Office under grant number 55104-EV and was supported by NSF EAR/IF #0929850.

ESURFD
2, 535–574, 2014

References

Abrahams, A. D. and Parsons, A. J.: Relation between sediment yield and gradient on debris-covered hillslopes, Walnut Gulch, Arizona, Geol. Soc. Am. Bull., 103, 1109–1113, 1991.

Abrahams, A. D., Parsons, A. J., Cooke, R. U., and Reeves, R. W.: Stone movement on hillslopes in the Mojave Desert, California: a 16 year record, Earth Surf. Proc. Land., 9, 365–370, 1984.

Abrahams, A. D., Parsons, A. J., and Hirsh, P. J.: Hillslope gradient-particle size relations: evidence for the formation of debris slopes by hydraulic processes in the Mojave Desert, J. Geol., 93, 347–357, 1985.

Birkeland, P. W.: Soils and Geomorphology, Oxford University Press, New York, 430 pp., 1999.

Cerda, A.: Effects of rock fragment cover on soil infiltration, interrill runoff and erosion, Eur. J. Soil Sci., 52, 59–68, 2001.

Chappell, A.: The limitations of using Cs-137 for estimating soil redistribution in semi-arid environments, Geomorphology, 29, 135–152, 1999.

Crouvi, O., Pelletier, J. D., and Rasmussen, C.: Predicting the thickness and aeolian fraction of soils in upland watersheds of the Mojave Desert, Geoderma, 195–196C, 94–110, 2013.

Dekner, R.: Intercomparison Run IAEA-326 and IAEA-327 Radionuclides in Soil, Analytical Quality Control Services, Vienna, Austria, 1996.

Dietrich, W. E. and Perron, T.: The search for a topographic signature of life, Nature, 439, 411–418, 2006.

Dietrich, W. E., Bellugi, D. G., Sklar, L. S., Stock, J. D., Heimsath, A. M. and Roering, J. J.: Geomorphic Transport Laws for Predicting Landscape form and Dynamics, in: Prediction in Geomorphology, edited by: Wilcock, P. R. and Iverson, R. M., American Geophysical Union, Washington, D. C., doi:10.1029/135GM09, 2013.

Douglas, I.: Man, vegetation and the sediment yields of rivers, Nature, 215, 925–928, 1967.

Fahnestock, P. B. and Novak-Echenique, P.: Soil Survey of National Training Center, Fort Irwin, California, USDA, NRCS, 730, 2000.

Freeman, T. G.: Calculating catchment area with divergent flow based on a regular grid, Comput. Geosci., 17, 413–422, 1991.

Govers, G., Van Oost, K., and Poesen, J.: Responses of a semi-arid landscape to human disturbance: a simulation study of the interaction between rock fragment cover, soil erosion and land use change, Geoderma, 133, 19–31, 2006.

ESURFD
2, 535–574, 2014

Granger, D. E., Riebe, C. S., Kirchner, J. W., and Finkel, R.: Modulation of erosion on steep granitic slopes by boulder armoring, as revealed by cosmogenic 26Al and 10Be, Earth Planet. Sc. Lett., 186, 269–281, 2001.
Griffiths, P. G., Hereford, R., and Webb, R. H.: Sediment yield and runoff frequency of small drainage basins in the Mojave Desert, USA, Geomorphology, 74, 232–244, 2006.
Heimsath, A., Dietrich, W., Nishiizumi, K., and Finkel, R. C.: Cosmogenic nuclides, topography, and the spatial variation of soil depth, Geomorphology, 27, 151–172, 1999.
Heimsath, A., Furbish, D. J., and Dietrich, W.: The illusion of diffusion: field evidence for depth-dependent sediment transport, Geology, 33, 949–952, 2005.
Hirmas, D. R., Graham, R. C., and Kendrick, K. J.: Soil-geomorphic significance of land surface characteristics in an arid mountain range, Mojave Desert, USA, Catena, 87, 408–420, 2011.
Kaste, J. M., Heimsath, A., and Hohmann, M.: Quantifying sediment transport across an undisturbed prairie landscape using cesium-137 and high resolution topography, Geomorphology, 76, 430–440, 2006.
Kaste, J. M., Heimsath, A., and Bostick, B. C.: Short-term soil mixing quantified with fallout radionuclides, Geology, 35, 243–246, 2007.
Kidron, G. J., Monger, C. H., Vonshak, A., and Conrod, W.: Contrasting effects of microbiotic crusts on runoff in desert surfaces, Geomorphology, 139–140, 484–494, 2012.
Lal, R.: Soil degradation by erosion, Land Degrad. Dev., 12, 519–539, 2001.
Mabit, L., Meusburger, K., Fulajtar, E., and Alewell, C.: The usefulness of 137Cs as a tracer for soil erosion assessment: a critical reply to Parsons and Foster (2011), Earth-Sci. Rev., 127, 300–307, 2013.
Nearing, M. A., Simanton, J. R., Norton, L. D., Bulygin, S. J., and Stone, J.: Soil erosion by surface water flow on a stony, semiarid hillslope, Earth Surf. Proc. Land., 24, 677–686, 1999.
Nearing, M. A., Kimoto, A., Nichols, M. H., and Ritchie, J. C.: Spatial patterns of soil erosion and deposition in two small, semiarid watersheds, J. Geophys. Res., 110, F04020, doi:10.1029/2005JF000290, 2005.
Nichols, K. K., Bierman, P. R., Hooke, R. L., Clapp, E. M., and Caffee, M.: Quantifying sediment transport on desert piedmonts using ^{10}Be and ^{26}Al, Geomorphology, 45, 105–125, 2002.
Nichols, K. K., Bierman, P. R., Eppes, M. C., Caffee, M., Finkel, R., and Larsen, J.: Timing of surficial process changes down a Mojave Desert piedmont, Quaternary Res., 68, 151–161, 2007.

ESURFD
2, 535–574, 2014

O'Farrell, C. R., Heimsath, A., and Kaste, J. M.: Quantifying hillslope erosion rates and processes for a coastal California landscape over varying timescales, Earth Surf. Proc. Land., 32, 544–560, 2007.
Owen, J., Amundson, R., Dietrich, W., Nishiizumi, K., Sutter, B., and Chong, G.: The sensitivity of hillslope bedrock erosion to precipitation, Earth Surf. Proc. Land., 36, 117–135, 2011.
Parsons, A. J. and Foster, R. C.: What can we learn about soil erosion from the use of 137Cs?, Earth-Sci. Rev., 108, 101–113, 2011.
Pelletier, J. D. and Rasmussen, C.: Geomorphically based predictive mapping of soil thickness in upland watersheds, Water Resour. Res., 45, W09417, doi:10.1029/2008WR007319, 2009.
Pelletier, J. D., McGuire, L. A., Ash, J. L., Engelder, T. M., Hill, L. E., Leroy, K. W., Orem, C. A., Rosenthal, S. W., Trees, M. A., Rasmussen, C., and Chorover, J.: Calibration and testing of upland hillslope evolution models in a dated landscape: Banco Bonito, New Mexico, USA, J. Geophys. Res., 116, F04004, doi:10.1029/2011JF001976, 2011.
Pimentel, D., Harvey, C., Resosudarmo, P., Sinclair, K., Kurz, D., McNair, M., Crist, S., Shpritz, L., Fitton, L., Saffouri, R., and Blair, R.: Environmental and economic costs of soil erosion and conservation benefits, Science, 267, 1117–1123, 1995.
Poesen, J. W., Torri, D., and Bunte, K.: Effects of rock fragments on soil erosion by water at different spatial scales: a review, Catena, 23, 141–166, 1994.
Quindos, L. S., Sainz, C., Fuente, I., Nicolas, J., Quindos, L., and Arteche, J.: Correction by self-attenuation in gamma-ray spectrometry for environmental samples, J. Radioanal. Nucl. Ch., 270, 339–343, 2006.
Reheis, M. C., Goodmacher, J. C., Harden, J. W., McFadden Leslie, D., Rockwell, T. K., Shroba, R. R., Sowers Janet, M., and Taylor, E. M.: Quaternary soils and dust deposition in southern Nevada and California, Geol. Soc. Am. Bull., 107, 1003–1022, 1995.
Renard, K. G. and Freimund, J. R.: Using monthly precipitation data to estimate the R-factor in the revised USLE, J. Hydrol., 157, 287–306, 1994.
Riebe, C. S., Kirchner, J. W., Granger, D. E., and Finkel, R. C.: Erosional equilibrium and disequilibrium in the Sierra Nevada, inferred from cosmogenic (super 26) Al and (super 10) Be in alluvial sediment, Geology, 28, 803–806, 2000.
Roering, J. J.: How well can hillslope evolution models "explain" topography?, Simulating soil transport and production with high-resolution topographic data, Geol. Soc. Am. Bull., 120, 1248–1262, 2008.

ESURFD
2, 535–574, 2014

Soil Survey Staff: Soil Taxonomy: a Basic System of Soil Classification for Making and Interpreting Soil Surveys, USDA Natural Resource Conservation Service Agriculture, US Government Printing Office, Washington DC, 1999.
Verheijen, F. G. A., Jones, R. J. A., Rickson, R. J., and Smith, C. J.: Tolerable vs. actual soil erosion rates in Europe, Earth-Sci. Rev., 94, 23–38, 2009.
Walling, D. E. and He, Q.: Improved models for estimating soil erosion rates from cesium-137 measurements, J. Environ. Qual., 28, 611–622, 1999.
Walling, D. E. and He, Q.: The Global Distribution of Bomb-derived 137Cs Reference Inventories, Report to the IAEA as a Contribution to the Co-ordinated Research Projects on Soil Erosion and Sedimentation, Department of Geography, University of Exeter, Exeter, 11, 2000.
Wischmeier, W. H. and Smith, D. D.: Predicting Rainfall Erosion Losses: a Guide to Conservation Planning, USDA/Science and Education Administration, US Gov. Printing Office, Washington, DC, 58, 1978.
Yair, A.: The role of topography and surface cover upon soil formation along hillslopes in arid climates, Geomorphology, 3, 287–299, 1990.
Yair, A. and Enzel, Y.: The relationship between annual rainfall and sediment yield in arid and semi-arid areas; the case of the northern Negev, Catena, 10, 121–135, 1987.
Yair, A. and Klein, M.: The infuence of surface properties on flow and erosion processes on debris covered slopes in an arid area, Catena, 1, 1–14, 1973.
Yair, A. and Kossovsky, A.: Climate and surface properties; hydrological response of small arid and semi-arid watersheds, Geomorphology, 42, 43–57, 2002.

ESURFD
2, 535–574, 2014

Table 1. The study sites characteristics.

Site	GM2	EPR2	EPR3	BRH
Lithology and geologic period*	Quartz monzonite, Cretaceous	Diorite, Jurassic	Granite, Cretaceous	Granite, Jurassic-Cretaceous
Average slope (°), aspect, and length (m) of transects	25, NE, 130	16, NW, 130	7, NNE, 65 13, SSW, 85	5, NNW, 125 10, SW, 55
Elevation (m)	1260	910	750	780
Average rock cover (> 0.5 m) (%) and stdev	33 ± 13	27 ± 23	0	0
Average vegetation cover (%) and stdev	52 ± 16	39 ± 9	20	10

* See Crouvi et al. (2013) for more details.

ESURFD
2, 535–574, 2014

Table 2. The ^{137}Cs inventories per soil profile for the reference and study sites.

	Reference profiles	GM2*	EPR2*	EPR3	BRH
Mean, Bq m^{-2}	834.0	571.2	373.4	188.6	141.6
Minimum, Bq m^{-2}	786.7	198.0	86.7	0	0
Maximum, Bq m^{-2}	881.2	881.2	786.7	451.3	508.2
Standard deviation, Bq m^{-2}	66.8	232.1	261.6	144.2	136.8
Coefficient of variation, %	8	26	33	32	27
Number of samples	2	8	8	14	16

* Statistics includes the reference profile.

ESURFD
2, 535–574, 2014

Table 3. Erosion rates per soil profile for the study sites.

	GM2[a]	EPR2[a]	EPR3[b]	BRH[b]
Mean, $t\,ha^{-1}\,yr^{-1}$	−3.60	−8.06	−17.90	−24.34
Minimum, $t\,ha^{-1}\,yr^{-1}$	−11.08	−17.45	<= −51.85	<= −51.85
Maximum, $t\,ha^{-1}\,yr^{-1}$	0.44	−0.45	−4.73	−3.82
Standard deviation, $t\,ha^{-1}\,yr^{-1}$	3.71	5.97	15.38	19.40
Number of samples	8	8	14	16

[a] Statistics includes the reference profile.
[b] Statistics includes profiles with no detectable ^{137}Cs activities that yield minimal erosion rates (two profiles at EPR2 and five at BRH). Thus, mean erosion rate for these sites is minimal estimation.

ESURFD
2, 535–574, 2014

Table 4. Percent of rock fragments (> 2 mm) in the soil profile (0–9 cm) for soils from the study sites.

	GM2	EPR2	EPR3	BRH
Mean, %	46.6	26.3	28.5	20.6
Minimum, %	40.3	9.8	16.3	0.9
Maximum, %	55.1	40.7	44.7	38.6
Standard deviation, %	5.2	10.2	8.6	10.3
Coefficient of variation, %	9.5	25.1	19.3	26.7
Number of samples	8	8	14	16

ESURFD
2, 535–574, 2014

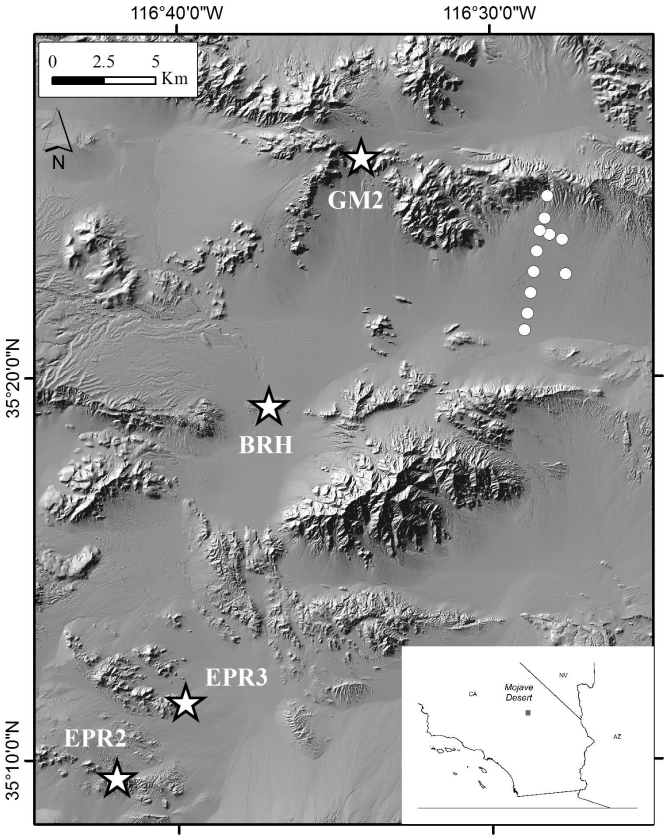

Figure 1. Location map of the four study sites (stars) in the southern part of Ft. Irwin, the Mojave Desert, southern CA. The location of previous estimations of millennial soil erosion rates are marked in circles (Nichols et al., 2007). Topography from the LiDAR data is presented as shaded relief image.

ESURFD
2, 535–574, 2014

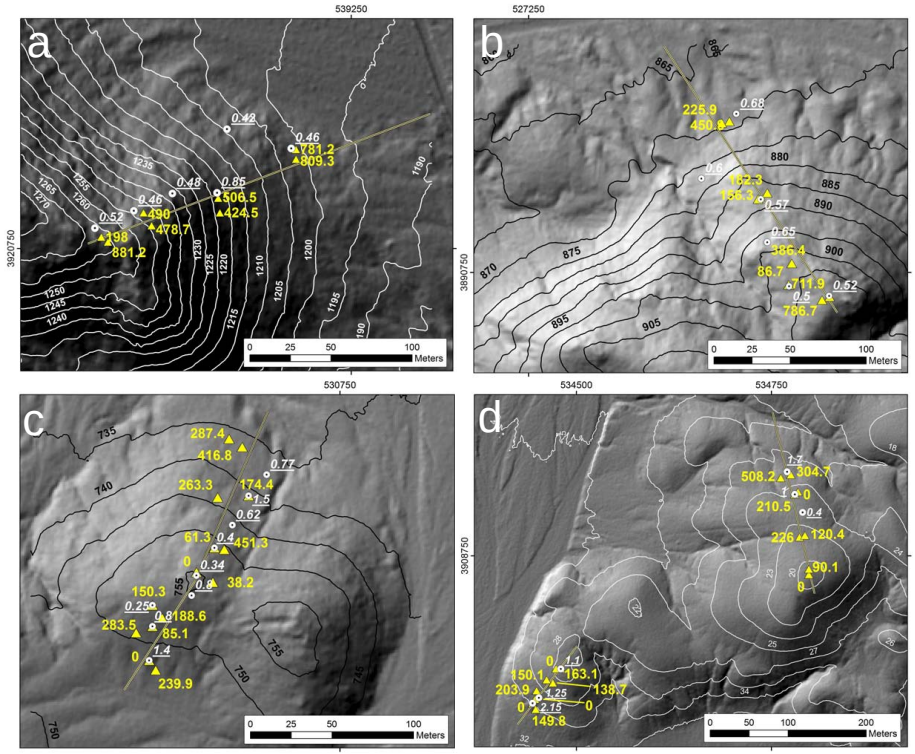

Figure 2. The spatial distribution of total ^{137}Cs inventories (Bq m^{-2}) per soil profile for each study site: **(a)** GM2, **(b)** EPR2, **(c)** EPR3, **(d)** BRH. Topographic transects are in yellow lines. Location and thickness (m) of studied soil pits (dug to bedrock) are in white circles. Topography from the LiDAR data is presented as contours and as shaded relief images.

ESURFD
2, 535–574, 2014

Controls on slope-wash erosion rates in the Mojave Desert

O. Crouvi et al.

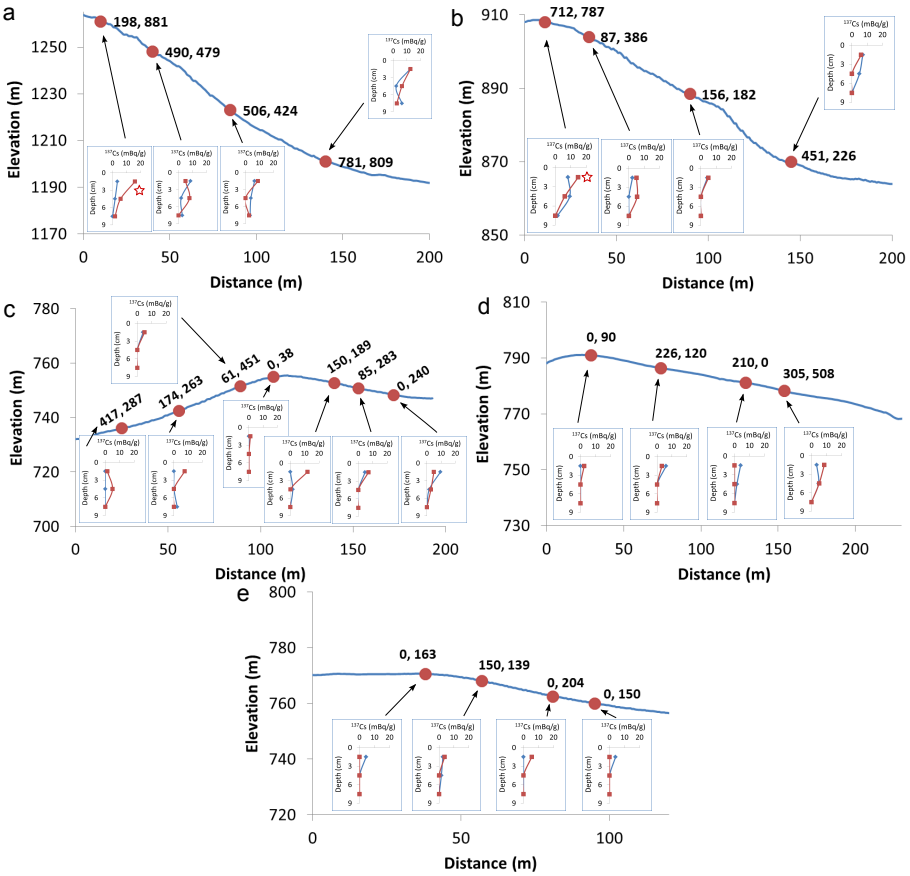

Figure 3. The distribution of total ^{137}Cs inventories (Bq m^{-2}) per soil pit along the hillslope for each study site: **(a)** GM2, **(b)** EPR2, **(c)** EPR3, **(d)** BRH north aspect, **(e)** BRH southwest aspect. Insets show depth profiles of ^{137}Cs activities (m Bq g^{-1}) for each soil profile. Profiles chosen for reference site are marked with *.

ESURFD
2, 535–574, 2014

Controls on slope-wash erosion rates in the Mojave Desert

O. Crouvi et al.

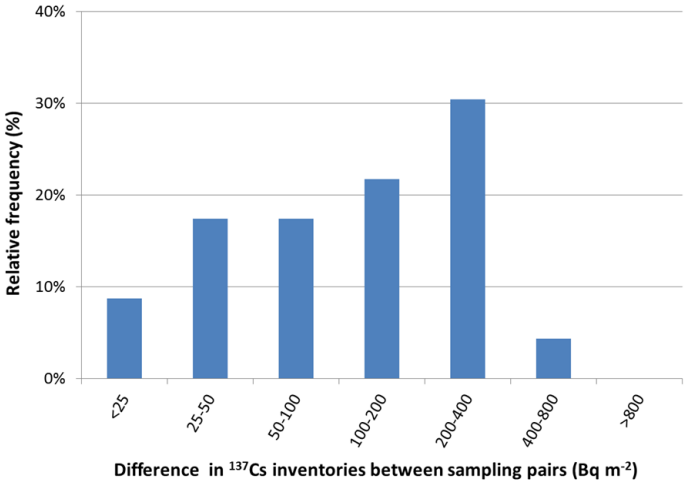

Figure 4. Relative frequency of difference in ^{137}Cs inventories (Bq m^{-2}) between sampling pairs for all study sites.

ESURFD
2, 535–574, 2014

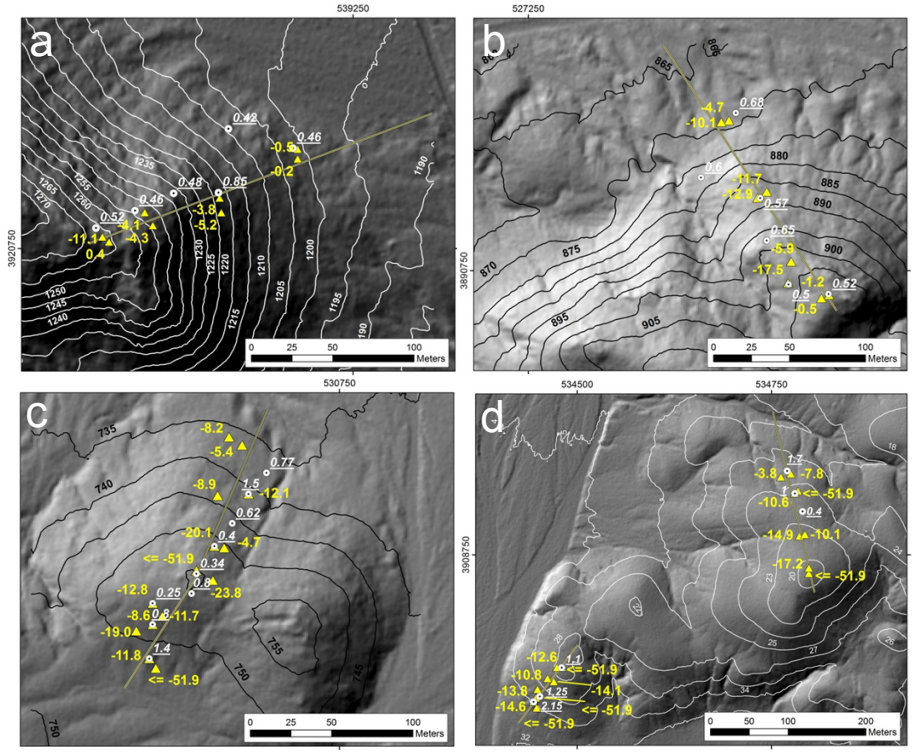

Figure 5. The spatial distribution of erosion and deposition rates ($t\,ha^{-1}\,yr^{-1}$) for each study site: **(a)** GM2, **(b)** EPR2, **(c)** EPR3, **(d)** BRH. All other features as in Fig. 2.

ESURFD
2, 535–574, 2014

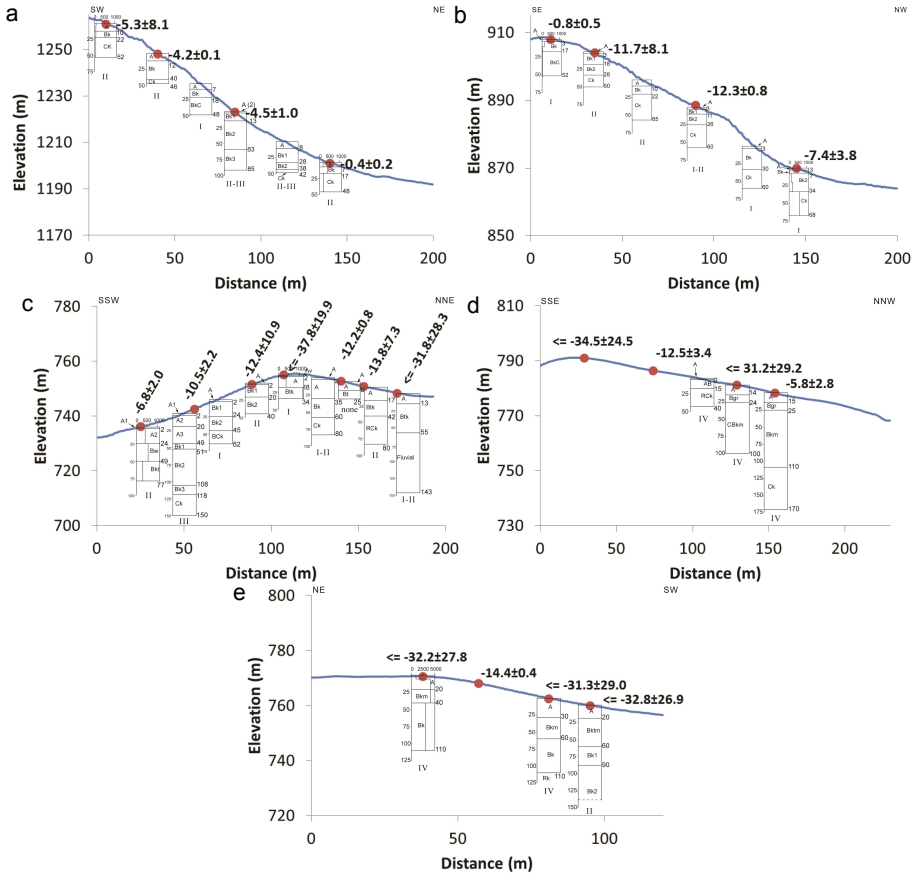

Figure 6. Erosion and deposition rates ($t\,ha^{-1}\,yr^{-1}$) with soil catena data for each study site: **(a)** GM2, **(b)** EPR2, **(c)** EPR3, **(d)** BRH north aspect, **(e)** BRH southwest aspect. The distribution of electrical conductivity values (EC) ($\mu S\,cm^{-1}$) with depth is presented for most of the summit and footslope profiles. Note scale difference for EC values at site BRH.

ESURFD
2, 535–574, 2014

Controls on slope-wash erosion rates in the Mojave Desert

O. Crouvi et al.

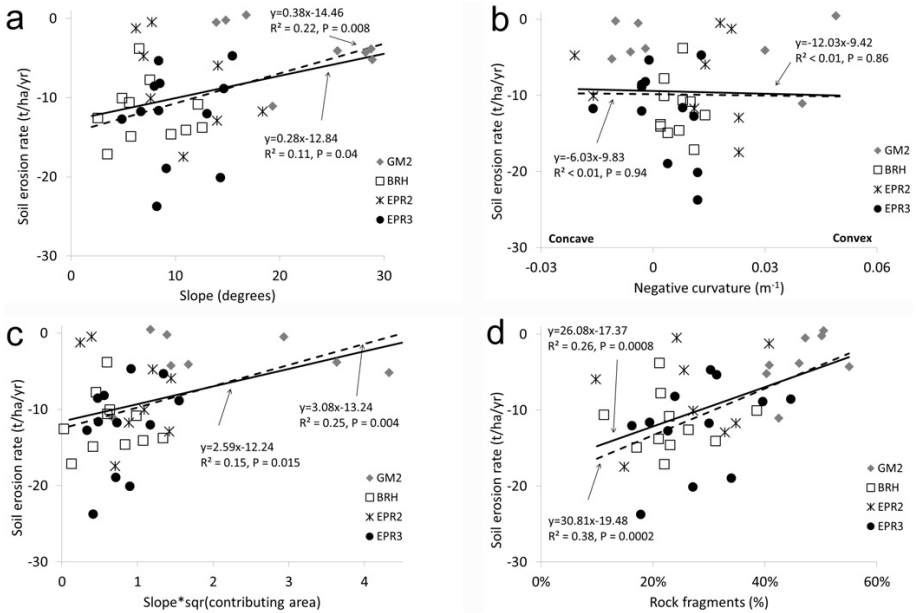

Figure 7. Relationships between calculated soil erosion and deposition rates ($t\,ha^{-1}\,yr^{-1}$) and slope **(a)**, curvature **(b)**, slope × sqrt(contributing area) **(c)** and rock fragments in soil **(d)**. Profiles with no detectable Cs (minimal erosion rates) are not considered in the regression analyses and do not appear in this figure. Regressions per site were found to be non-significant for all four examined variables. Regressions of all data points appear in black line; Regressions of all data points except site EPR2 appear in dashed line. Curvature presented is 1 m pixel; similar non-significant regressions were observed also for the 5 m pixel curvature data.

ESURFD
2, 535–574, 2014

Controls on slope-wash erosion rates in the Mojave Desert

O. Crouvi et al.

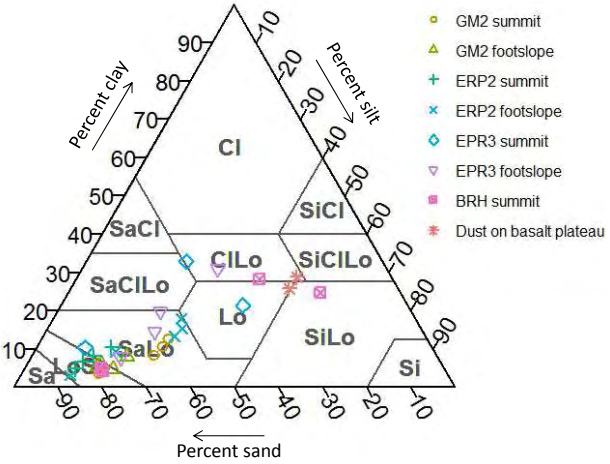

Figure 8. Particle size ternary plots and textural classes for the < 2 mm fraction of A and B horizons of the studies soils. Abbreviates are: Sa – sand, LoSa – loamy sand, SaLo – sandy loam, SaClLo – sandy clay loam, SaCl – sandy clay, Cl – clay, ClLo – clay loam, Lo – loam, SiCl – silty clay, SiClLo – silty clay loam, SiLo – silt loam, Si - silt

ESURFD
2, 535–574, 2014

Controls on slope-wash erosion rates in the Mojave Desert

O. Crouvi et al.